The Air-Sea Interface, Radio and Acoustic Sensing, Turbulence and Wave Dynamics, Marseille, 24-30. June 1993, edited by M. A. Donelan, W. H. Hui and W. J. Plant
RSMAS, University of Miami, 1996, doi: 10.5281/zenodo.14002

COMBINED WAVE AND FLOW FIELD VISUALIZATION FOR INVESTIGATION OF SHORT-WAVE/LONG-WAVE INTERACTION

Frank Hering and Dietmar Wierzimok
Institute for Environmental Physics, University of Heidelberg, Im Neuenheimer Feld 366, D-69120 Heidelberg, Germany

and

W. Kendall Melville and Bernd Jähne
Physical Oceanography Research Division, Scripps Institution of Oceanography, University of California - San Diego, La Jolla, CA 92093-0230, U.S.A.

Abstract. Short-waves modulated by long-waves have been investigated in the glass wave channel at Scripps Institution of Oceanography. Two series of mechanically generated wave trains of different amplitudes and wavelengths were produced consecutively in such a way that they superimpose 7.55 m from the wave maker. At this location, simultaneous records of wave slope images and the Lagrangian flow field were obtained, using an integrated two-camera setup, including particle-tracking and wave-slope instruments. With Digital Particle Tracking Velocimetry (DPTV), two-dimensional Eulerian and Lagrangian flow fields in an area of 17 by 20 cm^2 in the water were calculated. From the wave slope image sequences phase speed, local frequency, and local wave number were obtained.

1 Introduction

Long-wave/short-wave interaction is related to a number of important issues concerning the dynamics of the ocean and small scale air-sea interaction processes. Although theories have been developed over the last 40 years (Longuet-Higgins and Stewart, 1960; Longuet-Higgins, 1987; Zhang and Melville, 1990), direct experimental verification of many aspects of the theory is missing. Direct spatial measurements giving wavenumber modulation are lacking. In this paper a novel optical technique is described that combines two spatial measuring systems in one setup: wave slope imaging and flow visualization. Both systems have already been used individually for some time, but are now put together for the first time. The wave visualization provides all relevant parameters of the short wave: the local wave number, the frequency, and the phase speed as a function of the phase and amplitude of the long waves. From the flow field measurements, similar information is gained for the orbital velocities. In addition, two dimensional velocity fields and later vorticity fields can be derived, yielding mass flux and Reynold stresses. The aim of this paper is to describe the imaging techniques for simultaneous flow field and wave measurements.

2 Experimental Set-Up

2.1 The Wave Channel and Wave Generation

The experiments were conducted in the glass water channel at the Hydraulics Laboratory of Scripps Institution of Oceanography. This channel is 25 m long, 60 cm wide and 85 cm deep, and is filled to a depth of 60 cm. A computer

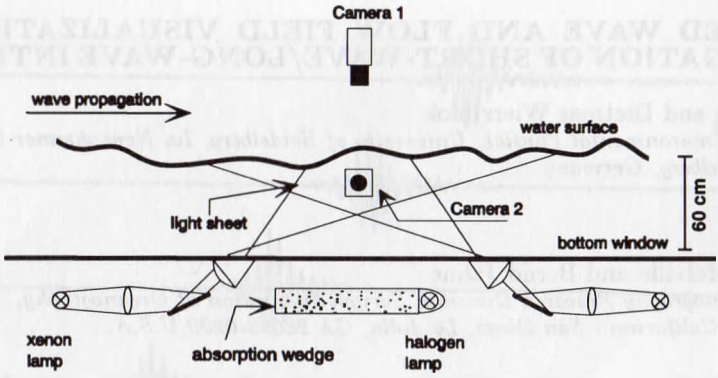

Fig. 1. Schematic of the optical instruments: **Camera 1** looking from above at a gradient illumination (Wave Visualization), and **Camera 2** observes a lightsheet, illuminating seeding particles (Flow Visualization).

controlled paddle generates mechanical waves. As the walls and bottom of this channel are glass, it is ideally suited for the installation of optical measuring devices. For wave generation, the method of Rapp and Melville (1990) was used. By taking the dispersion relation into account interacting wave trains can be generated using only one wave maker. The group velocity of the longer waves is greater than that of the shorter waves, e.g. $c_g[\lambda = 2.8\,\mathrm{m}] = 1.33\,\mathrm{m/s} > c_g[\lambda = 0.18\,\mathrm{m}] = 0.27\,\mathrm{m/s}$. First a short wave train and, after a certain delay, a long wave train were sent down the channel to superimpose at 7.55 m from the wave maker.

2.2 Flow Visualization

A 4 cm thick light sheet parallel to the main wave propagation direction is used to illuminate small ($50 - 150\,\mu\mathrm{m}$ in diameter) polystyrol (LATEX) seeding particles. Due to the presence of the absorption wedge this light sheet cannot be generated from below the channel. Thus it is produced at the sides of the wave visualization region and then coupled into the channel through a prism (see Fig. 1). An optical system consisting of a spherical lens ($f = 200\,\mathrm{mm}$) and a cylindrical lens ($f = 90\,\mathrm{mm}$) generates the light sheets. An immersion oil as an optical coupling medium links the prisms with the bottom window of the channel. As shown in Fig. 1 two illumination systems are combined to increase intensity and homogeneity in the image sector of $17 \times 20\,\mathrm{cm}^2$. The oblique illumination angle has been chosen so that most of the light is totally reflected at the water surface. Only in rare cases – for steep waves – is the light refracted in such a way that bright spots are observed in camera 1 for the wave slope imaging. This residual interference was eliminated by a blue Corion interference short wave pass filter (cut-off wavelength $\lambda = 550\,\mathrm{nm}$) in the light beam of the Xenon arc lamp and a red Schott glass filter (cut-on wavelength $\lambda = 600\,\mathrm{nm}$) on camera 1 (Fig. 1).

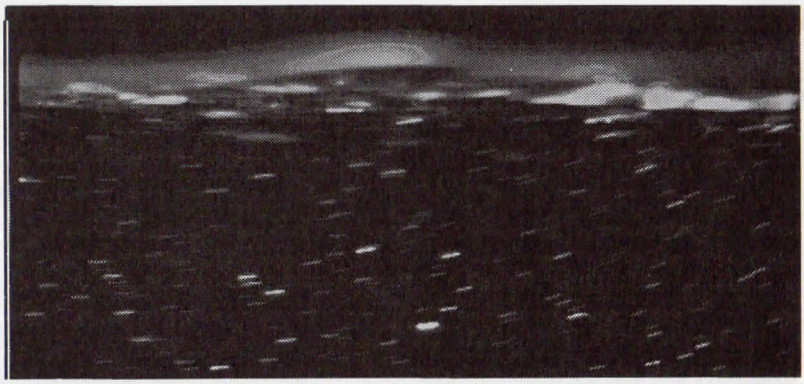

Fig. 2. Seeding particles beneath the water surface illuminated in a light sheet . Due to the exposure time of the camera particles in motion are visualized as streaks.

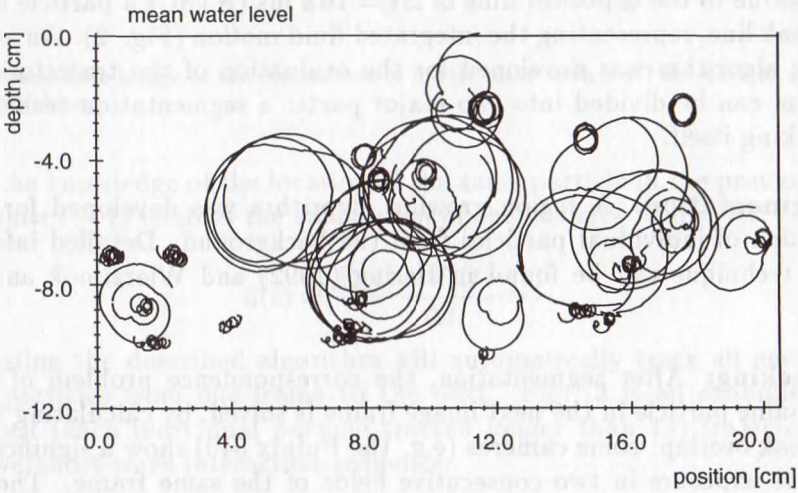

Fig. 3. Trajectories of a 3.0/0.7 Hz interaction sequence.

2.3 Imaging Slope Gauge (ISG)

A camera looks from above through the water surface onto an absorption wedge, which gives a gradient illumination (see camera 1 in Fig. 1). Depending on the slope of the wave, the camera observes different parts of the absorption wedge and therefore the slope of the wave is encoded as intensity in the images. Detailed information on this technique can be found in Jähne, 1993.

3 Determination of the 2-D flow vector field

In flow visualization one distinguishes between methods yielding the Eulerian and those giving Lagrangian flow field information. Eulerian flow field measurements (Adrian, 1991) are commonly based on imaging techniques, such as

Laser Speckle Velocimetry (LSV) or Particle Imaging Velocimetry (PIV). Particle Tracking Velocimetry (PTV) provides a Lagrangian representation of the flow field. Every seeding particle is traced along its trajectory within the light sheet, therefore the path $\vec{x}$ of a fluid element is a function of the initial starting point $\vec{x_0}$ and the elapsed time $t - t_0$.

$$\vec{x} = \vec{x}(\vec{x}_0, t - t_0) \tag{1}$$

$$\vec{v} = \vec{v}(\vec{x}_0, t - t_0) = \frac{\partial \vec{x}}{\partial t}(\vec{x}_0, t - t_0) \tag{2}$$

In contrast to the region-orientated PIV and LSV, tracking requires a relatively low seeding particle concentration (density ≤ 1000 particles per frame), as each particle is tracked individually. In addition a thick light sheet ($\approx 4\,\mathrm{cm}$) enables the reconstruction of particle trajectories in virtually hundreds of image frames. The particle motion is observed by a standard video CCD-camera (camera 2 in Fig. 1). Due to the exposure time of $\Delta t = 16.7\,\mathrm{ms}$ (NTSC) a particle is imaged as a streak line, representing the integrated fluid motion (Fig. 2). An automatic tracking algorithm was developed for the evaluation of the trajectories. This algorithm can be divided into two major parts: a segmentation technique and the tracking itself:

1. Segmentation: A region growing algorithm was developed for the discrimination of individual particles from the background. Detailed information on this technique can be found in Hering (1992) and Wierzimok and Hering (1992).

2. Tracking: After segmentation, the correspondence problem of identifying the same particle in the next image frame is solved, by calculating its image field streak overlap: some cameras (e.g. the Pulnix 640) show a significant overlap of the exposure in two consecutive fields of the same frame. The overlap of the exposure time yields a spatial overlap of the two corresponding streaks from one image to the next. This overlap can be increased artificially by dilating each object using morphological operators. In addition more features like the area, the sum of gray value and the interpolated vector field are calculated to minimize false correspondences. Wierzimok and Hering (1992) showed that the center of gray value $\vec{x}_c$ of an isotropic object represents the time-averaged two-dimensional location $\langle \vec{x} \rangle_{\Delta t}$, thus:

$$\vec{x}_c = \langle \vec{x} \rangle_{\Delta t} \tag{3}$$

where $\vec{x}_c$ is calculated from the sum of all n segmented pixels of a streak:

$$\vec{x}_c = \left(\frac{\sum_{i=1}^{n} x_i g(x_i, y_i)}{\sum_{i=1}^{n} g(x_i, y_i)}, \frac{\sum_{i=1}^{n} y_i g(x_i, y_i)}{\sum_{i=1}^{n} g(x_i, y_i)} \right). \tag{4}$$

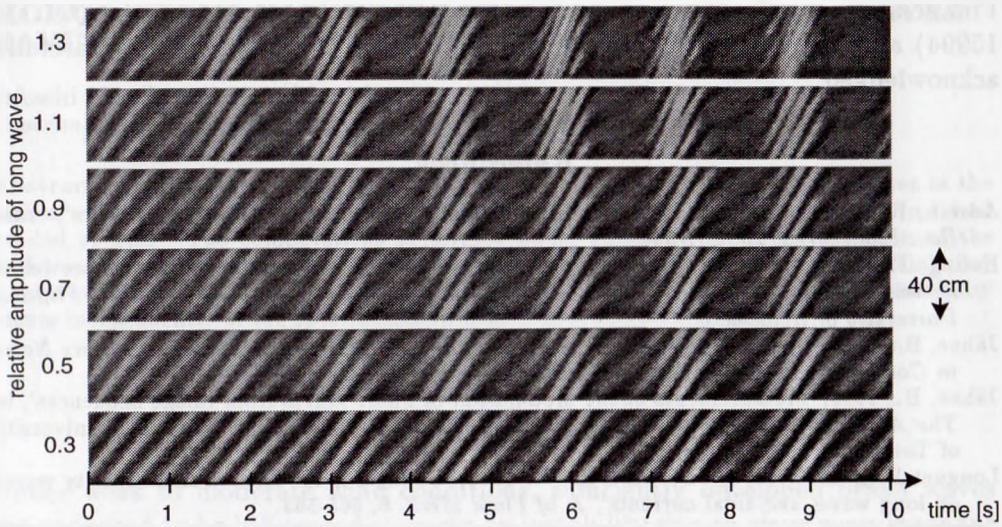

Fig. 4. Space-time-image of the interaction of a 3 Hz wave with a 0.7 Hz wave of amplitudes as indicated above.

Now the knowledge of the location of the same particle in the previous frame (at the time $t-1$) enables the calculation of the velocity field $\vec{u}(t)$:

$$\vec{u}(t) \approx \frac{\vec{x}_c(t) - \vec{x}_c(t-1)}{\Delta t}. \tag{5}$$

Repeating the described algorithm will automatically track all encountered seeding particles from one frame to the next. Fig. 3 is an example of only the longest (each individual particle tracked longer than 1*s*) trajectories of a long-wave/short-wave interaction sequence.

4 Determination of the Modulation from the Wave Measurement

With the previously described wave visualization, image series were taken of long-wave/short-wave interactions. From these images space-time images (xt-images) were generated, by taking the same line out of each picture of the series and building consecutively a new image, see Fig. 4. Spatio-temporal images are a powerful tool for the detection of motion and the speed of motion. An object moving with uniform speed corresponds to a diagonal line in a xt-image, while a non moving object leaves a horizontal line as its signature. The determination of the local orientation therefore is a direct measure of the local phase speed, (see Jähne, 1993). Fig. 4 shows several xt-images of the interaction of a 3 Hz wave with a 0.7 Hz wave of different amplitudes. Hilbert filters were used for the determination of the local frequency and wave number. A Hilbert filter shifts the phase of a periodic signal by $\pi/2$ without changing its amplitude. The image processing techniques involved are described in more detail by Jähne (1996).

5 Acknowledgements

Financial support for this research from the National Science Foundation (OCE91 15994) and the German Science Foundation DFG (Wi 1029/2-1) is gratefully acknowledged.

References

Adrian, R. J.: 1991, 'Particle-Imaging Techniques for Experimental Fluid Mechanics', *Ann. Rev. Fluid Mech.* **23**, 261-304.

Hering, F.: 1992, 'Messung von Transportgeschwindigkeiten in winderzeugten Wasserwellen mittels Digitaler Bildfolgenanalyse', *Diploma thesis, Institute for Environmental Physics, University of Heidelberg.*

Jähne, B.: 1993, 'Spatio-Temporal Image Processing, Theory and Applications', *Lecture Notes in Computer Science*, Springer, JSI, Berlin.

Jähne, B.: 1996, 'Measurements of the Modulation of Short Waves from Image Sequences', in *The Air-Sea Interface*, Eds. M. A. Donelan, W. H. Hui, and W. J. Plant, The University of Toronto Press, Toronto.

Longuet-Higgins, M. S., and Stewart, R. W.: 1960, 'Changes in the form of short gravity waves on long waves and tidal currents', *J. of Fluid Mech.* **8**, 565-583.

Longuet-Higgins, M. S.: 1987, 'The propagation of short surface waves on longer gravity waves', *J. of Fluid Mech.* **177**, 293-306.

R. J., and Melville, W. K.: 1990, 'Laboratory Measurements of Deep-Water Breaking Waves', *Phil. Trans Roy. Soc. Lond.* **A331**, 735-800.

Wierzimok, D., and Hering, F.: 1992, 'Quantitative Imaging of Transport in Fluids with Digital Particle Tracking Velocimetry', *Proceedings Int. Seminar on Imaging in Transport Processes, Athens.*

Zhang, J., and Melville, W. K.: 1990, 'Evolution of Weakly Nonlinear Short Waves Riding on Long Gravity Waves – Derivation of the Nonlinear Schrödinger Equation and its Steady Solution', *J. of Fluid Mech.* **214**, 321-346.